SAXS and DSC Studies of the Crystallization and Melting Phenomena of Poly(ε-caprolactone)

B. Heck,[2] E. R. Sadiku,[1]* G. R. Strobl[2]

[1]Institute for Polymer Science, University of Stellenbosch, Private Bag X1 Matieland 7602, Republic of South Africa

[2]Faculty of Physics, University of Freiburg, Hermann-Herder-Straβe 3, D-79104 Freiburg, Germany

SUMMARY: The relationships between the crystallization temperature, T_c, the crystal thickness, d_c and the melting peak temperature, T_m of poly(ε-caprolactone)have been determined by carrying out time- and temperature-dependent small angle x-ray scattering experiments. A two-step melting has been suggested, resulting in the occurrence of two well defined independent boundary lines, indicating the transformation from melt into the partially crystalline state. For crystallization temperatures lower than 40°C, during heating, more pronounced peak shifts are observed with the final melting of the crystallites having the same thickness of $d_c \approx 7$ nm. In this region, it is evident that crystals have relatively good stabilities, since they have fairly uniform thickness. At higher temperatures, above 40°C, T_m increases with T_c, together with the thickness. The transformation of the melt into the partially crystalline state depicts a two-step process, beginning with the formation of a well defined initial structure with lower order, which is subsequently stabilized.

Introduction

An important parameter in the understanding of the crystalline state of polymers is the equilibrium melting temperature, T_m^θ, which defines the point at which infinitely large crystals melt[1)]. This is so because of the dependence of the crystallization kinetics on the supercooling, i.e. the difference between this parameter and the crystallization temperature, T_c. Within the range of accessible crystallization temperatures examined in this study, crystal

 CCC 1022-1360/00/$ 17.50+.50/0

thicknesses are inversely proportional to the supercooling below a well-defined characteristic temperature. Observations demonstrate that crystal thicknesses are not determined exclusively by the supercooling below the respective melting point of the polymer under investigation[2, 3], but also on the absolute temperature chosen for crystallization. Melting, commences immediately, at just above the crystallization temperature and then extends right up to the melting peak. There is no change in the thickness of the crystallites throughout the full melting range. Therefore, the stability of crystallites is certainly not a function of the crystal thickness only, but is also affected by additional controlling factors. In the beginning, there is the emergence of an initial form, which is just stable at T_c. This form then becomes stabilized at T_c and also during heating, but finally turns into layer-like crystallites, which melt at T_m. Considering the character of the structure at the initial state, we found evidence that it may be envisaged as an assembly of crystal blocks. The block dimensions with an edge length along the chain direction equal to the thickness of the final lamellae and values of the same order of magnitude in the lateral directions set them just at the limit of their stability. The lamellae then arise from a merging of the blocks and this provides the observed stabilization at constant d_c.

The focus of this study was initially on the crystal thickness, but of equal importance is the degree of crystallinity and its dependence on the crystallization temperature. While the thickness of the crystallites changes on varying the crystallization temperature, their global volume fraction remains constant, thus constituting an invariant parameter. Primary crystallization produces some imperfect crystals, which are subsequently stabilized by structural relaxation processes, that affect both interior and surface regions[4-7]. However, a new primary crystallization can be avoided since the combination of small-angle x-ray scattering and dilatometry was possible, as the dilatometric measurements were performed directly after the SAXS experiments on the same sample. Analysis of scattering data of partially crystalline polymers is usually done by assuming a one-dimensional model of stacked parallel crystallites, following which the derivation of the corresponding one-dimensional interface distribution function or correlation function is carried out, neglecting the contributions of the edges. The crystallization and melting phenomena of poly(ε-

caprolactone) were looked at, with a view of shedding more light on these characteristics, since there is little available literature on the material, unlike the polyolefins.

Experimental Part

Poly(ε-caprolactone) sample was purchased from Aldrich Chemical Co. It has a number-average molecular weight, M_n,of 425 000 with a distribution of 1.5. A Kratky camera was attached to a conventional Cu-K_α x-ray source having a temperature controlled sample holder. Using a position-sensitive metal wire detector consisting of a scintillation counter and a PC-controlled step system, intensity curves of sufficient accuracy were registered within a few minutes counting time. A deconvolution exercise was carried out by employing the desmearing algorithm developed by Strobl[8] since the camera is equipped with a slit focus. Employing a moving slit method, measurements of absolute intensities were recorded.
To complement the SAXS experiments, a Perkin Elmer Model DSC4 with a mercury filled dilatometer was also used to monitor the kinetics of crystallization and melting of the sample. A heating rate of $10Kmin^{-1}$ was employed for the DSC experiments.

Theory and Data Analysis

A comprehensive analysis of SAXS data for the determination of crystal thickness has been described elsewhere[2, 6, 7]. Following the determination of the primary beam intensity with the moving slit system, the desmeared scattering curves were obtained in absolute values as differential cross sections per unit volume, $\sum(s)$. The quantity s denotes the modulus of the scattering vector, which is related to the scattering angle, 2θ, by:

$$s = \frac{2}{\lambda}\sin\frac{\theta}{2} \qquad (1)$$

where λ is the x-ray wavelength

$$\text{and } \lim_{s\to\infty}\sum(s) = r_e^2 \frac{P}{(s/2\pi)^2} \qquad (2)$$

where the parameter r_e is the classical electron radius, $r_e = 2.81\text{x}10^{-15}$ m and P is the Porod parameter.

The scattering intensity, I(s) is related to the one-dimensional electron density autocorrelation function, $K(z)$. Knowing $\sum(s)$ and $K(z)$, its second derivative, $K''(z)$ which gives the interface distance distribution function can be calculated by directly applying the Fourier relations. The estimation of the crystal thickness in semicrystalline polymers using the one-dimensional correlation function is a well established[9] technique. Scattering density correlation functions were computed from the SAXS data and the thickness of the crystalline region was determined from the extrapolated linear region of the density correlation function. From the scattering intensity, I(s), the correlation function $K(z)$ can be calculated by:

$$K(z) = 2\int_0^\infty 2\pi s^2 I(s)\cos(2\pi sz)ds \qquad (3)$$

The second derivative of the correlation function, $K''(z)$, depicts the distribution of distances between interfaces[10] and it is represented by:

$$K''(z) = \frac{O_s}{2}\Delta\rho^2\left[h_a(z) + h_c(z) - 2h_{ac}(z) + h_{aca}(z) + h_{acc}(z).....\right] \qquad (4)$$

where O_s is the interface per volume, the so-called "specific inner surface" of the interface separating the crystalline and the amorphous regions. It is strongly related to the first derivative $K(z)$ and $\Delta\rho$ is the difference in density. The expression in the square bracket comprises a series of distribution functions with subscripts indicating which phases (amorphous or crystalline) are to be accessed when traversing from one phase to another. However, only the first three contributions are of practical importance to $K''(z)$ and they represent the distributions of the thickness of the amorphous and the crystalline layers (h_a and h_c) and of the sum of both, resulting in the long period, L (h_{ac}). Should the structure possess sharp phase boundaries between the crystalline and amorphous regions and within the resolution of SAXS experiments, the asymptotic behavior of the intensity, I(s), is described by the Porod's law:

$$\lim_{s\to\infty} I(s) = \frac{P}{s^4}, \text{ with } P = \frac{O_s \Delta\rho^2}{8\pi^3} \qquad (5)$$

and $K''(z)$ follows from the scattering intensity I(s) as:

$$K''(z) = 16\pi^3 \int_o^\infty ds\left[\lim_{s\to\infty} I(s)s^4 - I(s)s^4\right]\cos(2\pi sz) \qquad (6)$$

Equation 6 can be successfully applied to experimental data following the subtraction of the superposed background scattering caused by density fluctuations within both phases. It is done by fitting the data in the region of high scattering vectors by a superposition of the Porod scattering. To reduce the effect of noise, a smoothing of the data is carried out.

Results and Discussion

Following the melting in the Kratky camera, a sample was kept in the melt for some time and later cooled in the camera as fast as possible to the chosen crystallization temperature in the range between 36 and 58°C. To ensure that crystallization did not start before isothermal conditions were achieved, the intensity of the beam was carefully monitored. After isothermal condition had been reached, the development of the structure was monitored by time-dependent small angle x-ray experiments. Figure 1 shows an example of the result of an experiment carried out at the crystallization temperature T_c = 44°C. It is the absolute SAXS intensity plot versus scattering vector; the background due to density fluctuations is yet to be corrected.

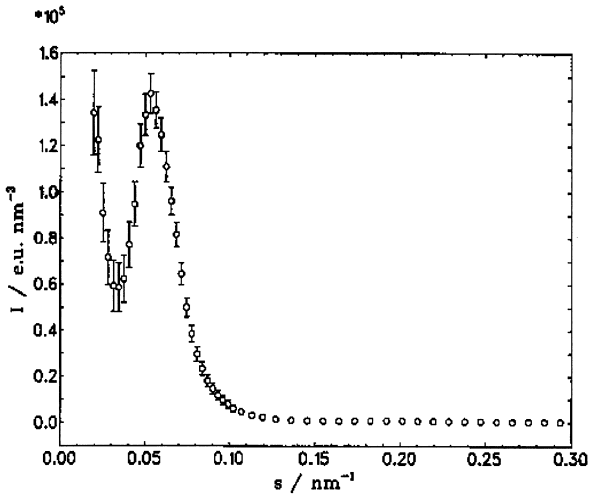

Fig. 1: SAXS intensity plot versus scattering vector, s, for poly(ε-caprolactone).

Figure 2 represents the desmeared SAXS intensity, $I(s)s^2$, curve versus scattering vector, s, after the completion of crystallization The electron density correlation function, $K(z)$, as it evolves as a function of time, is represented in Figure 3a, and Figure 3b indicates the corresponding correlation functions, $K(z)$, following smoothening. It represents the structure evolution in the course of isothermal crystallization at this temperature. Measurements taken at about 420 seconds indicates a crystal thickness of about 7 nm.

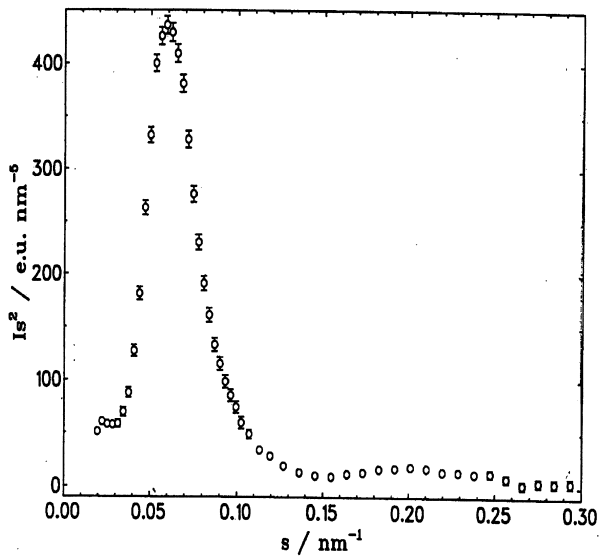

Fig. 2: Desmeared SAXS intensity $I(s)s^2$ versus scattering vector, s after the subtraction of the background intensity.

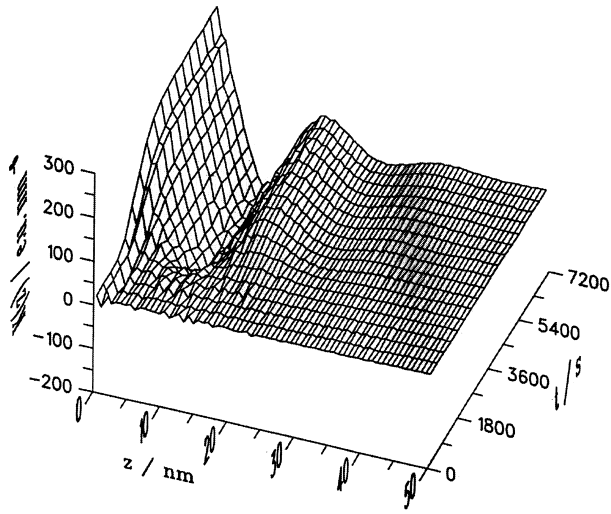

Fig. 3a: Isothermal crystallization of poly(ε-caprolactone) at T_c = 44°C, monitored by time-dependent SAXS.

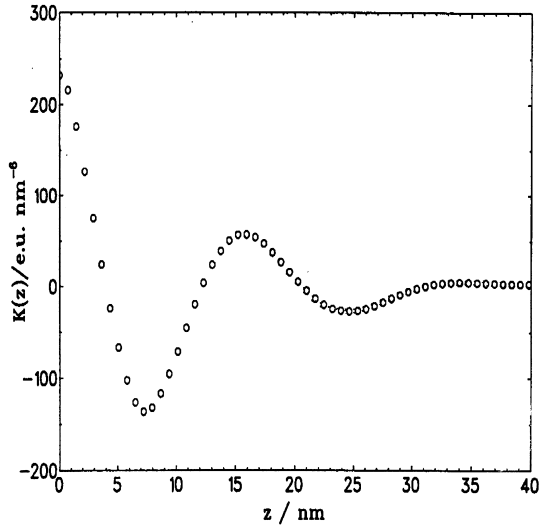

Fig. 3b: Cosine-transform correlation function computed from the SAXS crystallization data for poly(ε-caprolactone).

At the initial stage of crystallization, $K(z)$ is seen by the "self-correlation triangle" only, as indicative of individual crystallites. The width of the base of the triangle gives an indication of the crystallite thickness, d_c which amounts to about 6.96 nm. Then, as crystallization continues, a stack of crystallites is formed. The peak at around 15 nm gives the long spacing of the final structure. Similar or equivalent information can be derived from the second derivative, $K''(z)$. Equation 16 relates $K''(z)$ to the distribution of distances between interfaces in the stack.

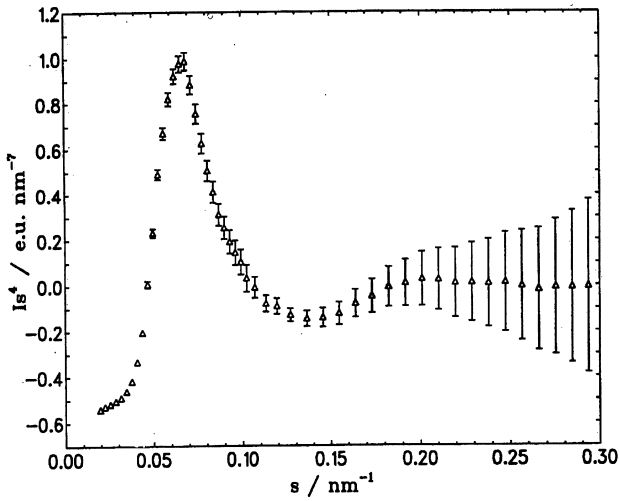

Fig. 4: Desmeared scattering intensity, $I(s)s^4$ obtained during the isothermal crystallization following the subtraction of the background intensity.

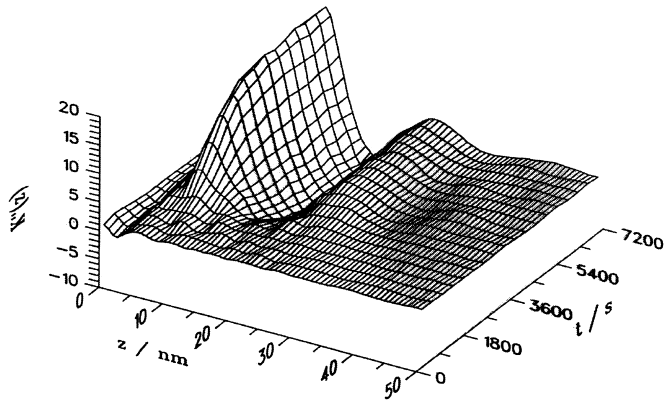

Fig. 5: Isothermal crystallization of poly(ε-caprolactone) showing the second derivative, $K''(z)$ gives the distribution function of interface distances, z.

Figure 4 shows the scattering intensity $I(s)s^4$ following the subtraction of the background scattering due to density fluctuations. The halos and the Lorentz polarization effects and the second derivative, $K''(z)$ as a function of time, is represented in Figure 5. A dominant ridge reflecting the crystallites and their thickness is located with its maximum at about 6.96 nm. In $K''(z)$, the long spacing, L shows up at a maximum, located at 15 nm. Figure 6 shows the $K''(z)$ following smoothening and a noise reduction exercise.

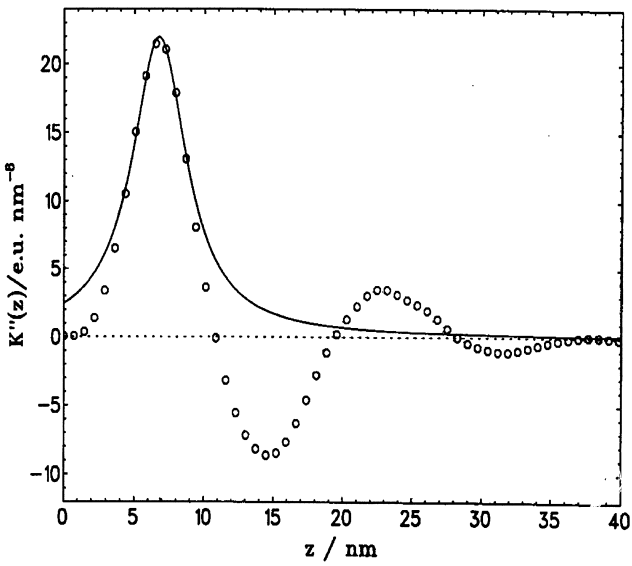

Fig. 6: Cosine-transform function $K''(z)$ calculated from a series of measurements during the SAXS isothermal crystallization of poly(ε-caprolactone) at T_c=44°C.

Figures 7a and b show the representative DSC isothermal crystallization of poyl(ε-caprolactone) as functions of temperature and time, respectively. At these two crystallization temperatures, maximum crystallization rates occur at 57.85°C and 432 seconds, respectively. Figure 8 shows the DSC melting endotherm with the melting peak occurring at about 58°C, with an enthalpy heat of fusion of $\approx 67 Jg^{-1}$.

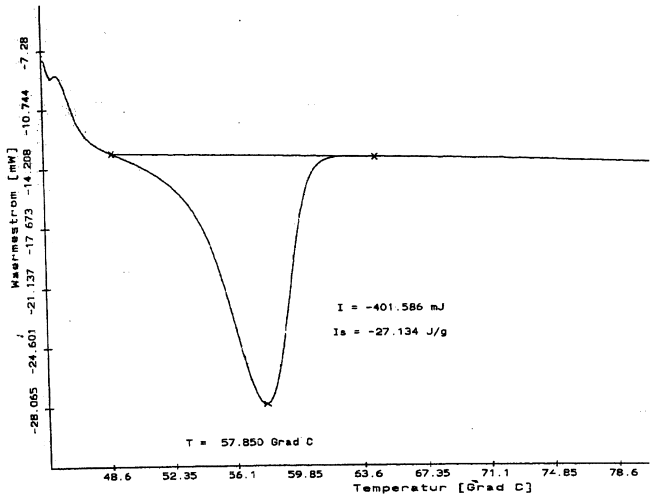

Fig. 7a: DSC isothermal crystallization plot of poly(ε-caprolactone) as a function of temperature.

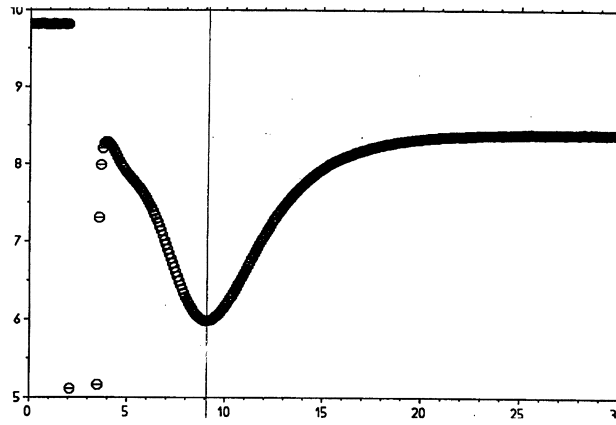

Fig. 7b: DSC isothermal crystallization poly(ε-caprolactone) as a function of time (in minutes), $T_c = 40^oC$.

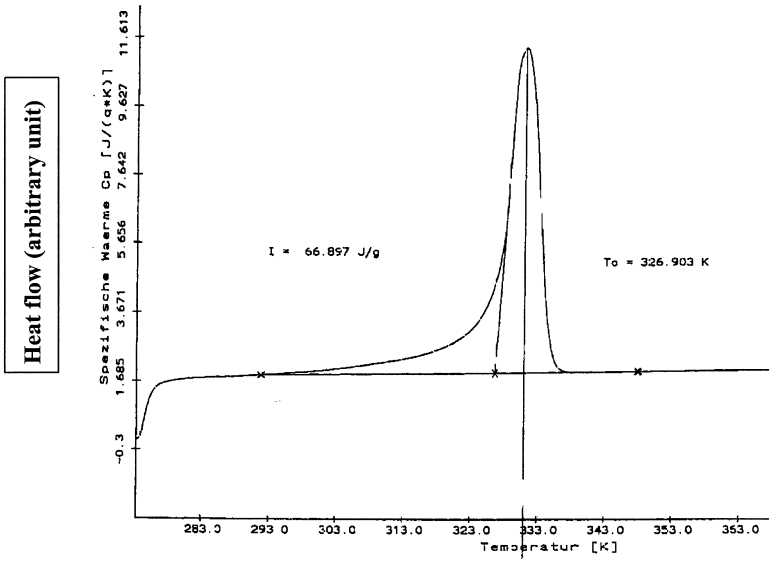

Fig. 8: DSC melting thermogram of poly(ε-caprolactone) as a function of temperature.

Figure 9 shows the Hoffman-Weeks plot obtained with data from the DSC. Figure 10 is the Gibb-Thomson plot obtained for both melting and crystallization experiments with the aid of SAXS. Extrapolations of data from both techniques to $d_c^{-1} = 0$ nm hovers around a value of equilibrium melting temperature, $T_m^{\theta} \approx 72.8°C$, which is not too far from literature value of around 70°C. Heck et al[2] reported that, rather than obtaining the equilibrium melting temperature using the popular Hoffman-Weeks plots, one most often obtains, erroneously, the characteristic temperature, T_{cf}.

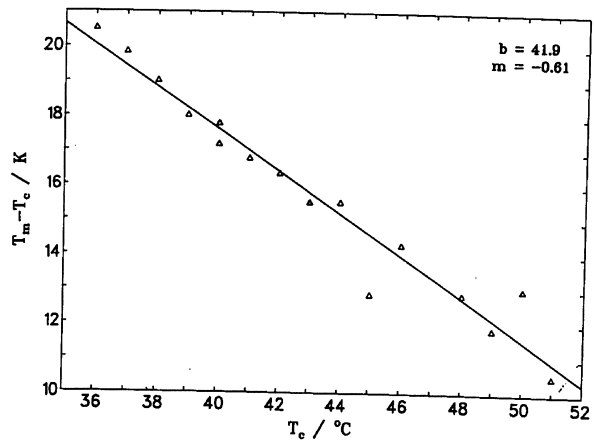

Fig. 9: Hoffman-Weeks plot for poly(ε-caprolactone).

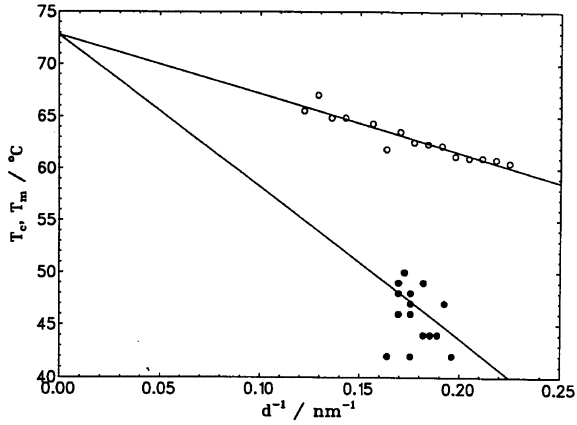

Fig. 10: Gibbs-Thomson plot plot for poly(ε-caprolactone) (open symbol, T_m and filled symbol, T_c).

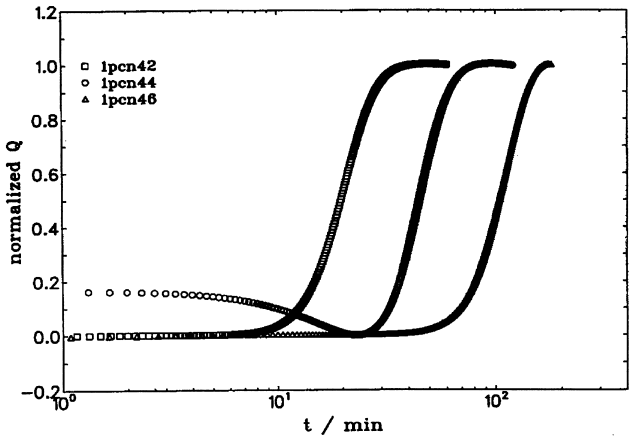

Fig. 11: SAXS kinetics of isothermal crystallization of poly(ε-caprolactone) at T_c = 42°C (□), 44°C (○) and 46°C (Δ) followed by the time dependence of the Porod coefficient.

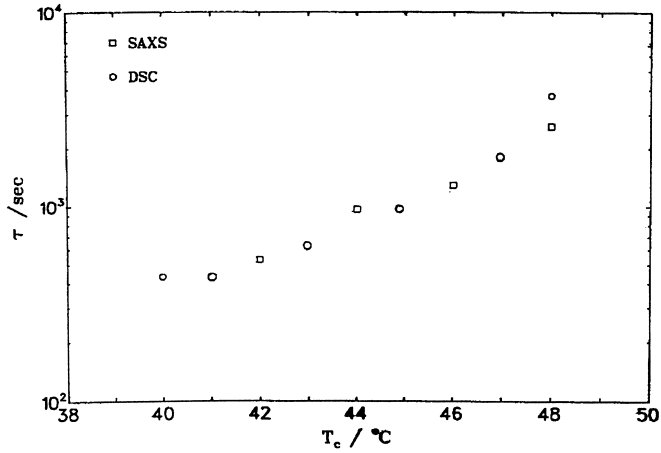

Fig. 12: Isothermal crystallization times at different crystallization temperatures, T_cs, taken from Figure 11 (□) and determined by DSC (○).

Figure 11 shows some selected SAXS kinetics of isothermal crystallization curves Q(t) at the indicated crystallization temperatures T_cs = 42, 44 and 46°C, followed by the time dependence of the normalized Porod coefficient. Figure 12 is the derived dependence of the characteristic crystallization time, $\tau(T_c)$ taken from Figure 11. Within the accessible range of temperature, isothermal crystallization times increase with increase in the crystallization temperature, as shown in Fig. 12.

Conclusion

In supercooled polymer melt, the formation of a semicrystalline state is believed to be a two-stage process. The formation of the initial state of lower order as defined by the crystallization line is thought to have been passed over into the final lamella structure via the Gibbs-Thomson melting line, with the stability attained without any significant detectable changes in d_C. Especially significant is the Gibbs-Thomson crystallization line which explicitly relates d_c^{-1} with T_c. The intersection of the melting and crystallization lines, following extrapolation to d_c^{-1} = 0 nm, occurred at about 73°C, which is close to the often quoted equilibrium melting temperature, T_m^{θ} of ≈ 70°C, frequently and erroneously obtained from the Hoffmann-Weeks plot.

1. M-H. Kim, P.J. Phillips, J.S. Lin, *J. Polym. Sci.*, vol. 38, 154-170 (2000)
2. B. Heck, T. Hugel, M. Iijima, E. Sadiku, G. Strobl, *New Journal of Physics*, 1, 17.1-17.29 (1999) (http://www.njp.org/)
3. T. Hugel, G. Strobl, R. Thomann, *Acta Polymerica*, 50, 214 (1999)
4. G. R. Strobl, *The Physics of Polymers*, Springer, Berlin, 1997
5. T. Albrecht, G. R. Strobl, *Macromolecules*, 29, 783-785 (1996)
6. J. Schmidtke, G. Strobl, T. Thurn-Albrecht, *Macromolecules*, 30, 5807 (1997)
7. T. Albrecht, G. Strobl, *Macromolecules*, 28, 5267-5273 (1995)
8. G. R. Strobl, *Acta Crystallogr.*, A26, 367, (1970)
9. G. R. Strobl, M. Schneider, *J. Polym. Sci.*, 18, 1343 (1980)
10. W. Ruland, *Colloid Polymer Sci.* 255, 417 (1977)